Accepted Manuscript

In vitro and *in vivo* studies of gold(I) azolate/phosphane complexes for the treatment of basal like breast cancer

Valentina Gambini, Martina Tilio, Eunice Wairimu Maina, Cristina Andreani, Caterina Bartolacci, Junbiao Wang, Manuela Iezzi, Stefano Ferraro, Anna Teresa Ramadori, Oumarou Camille Simon, Stefania Pucciarelli, Guojun Wu, Q. Ping Dou, Cristina Marchini, Rossana Galassi, Augusto Amici

PII: S0223-5234(18)30492-6

DOI: 10.1016/j.ejmech.2018.06.002

Reference: EJMECH 10472

To appear in: *European Journal of Medicinal Chemistry*

Received Date: 8 May 2018

Revised Date: 31 May 2018

Accepted Date: 1 June 2018

Please cite this article as: V. Gambini, M. Tilio, E.W. Maina, C. Andreani, C. Bartolacci, J. Wang, M. Iezzi, S. Ferraro, A.T. Ramadori, O.C. Simon, S. Pucciarelli, G. Wu, Q.P. Dou, C. Marchini, R. Galassi, A. Amici, *In vitro* and *in vivo* studies of gold(I) azolate/phosphane complexes for the treatment of basal like breast cancer, *European Journal of Medicinal Chemistry* (2018), doi: 10.1016/j.ejmech.2018.06.002.

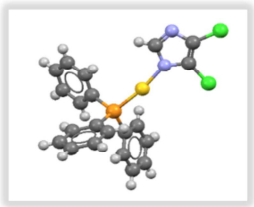

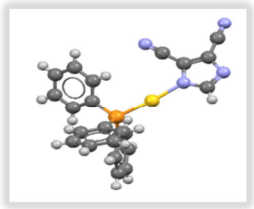

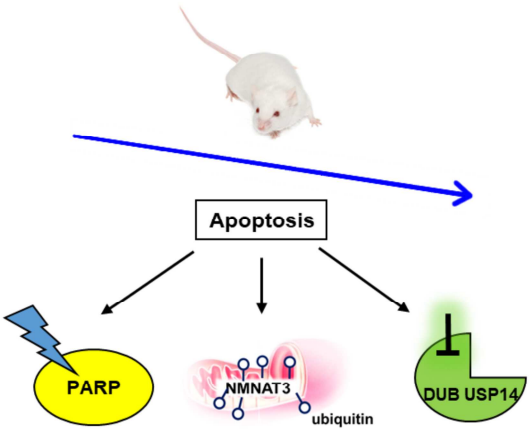

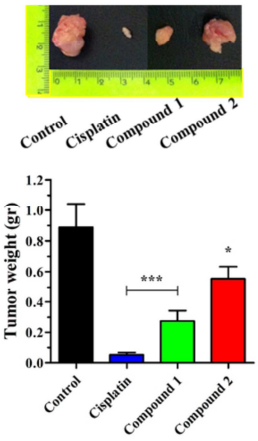

In vitro and *in vivo* studies of gold(I) azolate/phosphane complexes for the treatment of Basal Like Breast Cancer

Valentina Gambini[1,†], Martina Tilio[1,†], Eunice Wairimu Maina[1], Cristina Andreani[1,], Caterina Bartolacci[1,], Junbiao Wang[1], Manuela Iezzi[2], Stefano Ferraro[3], Anna Teresa Ramadori[3], Oumarou Camille Simon [3], Stefania Pucciarelli[1], Guojun Wu[4], Q. Ping Dou[4], Cristina Marchini[1,*], Rossana Galassi[3,†,*], Augusto Amici[1,†]

[1] *School of Biosciences and Veterinary Medicine, University of Camerino, Camerino, 62032, Italy.*

[2] *Aging Research Centre, G. d'Annunzio University, Chieti, 66100, Italy.*

[3] *School of Science and Technology, Chemistry Division, University of Camerino, Camerino, I-62032, Italy.*

[4] *Barbara Ann Karmanos Cancer Institute, Department of Oncology, School of Medicine, Wayne State University, Detroit, MI 48201, USA.*

[*] To whom correspondence should be addressed: Rossana Galassi, School of Science and Technology, Chemistry Division, Via Sant'Agostino, 1 I-62032, Camerino, Italy Tel:+39 0737 402243; Email: rossana.galassi@unicam.it; Cristina Marchini, School of Biosciences and Veterinary Medicine, via Gentile III Da Varano, University of Camerino, Camerino, 62032, Italy. Tel: +39 0737 403275; Email: cristina.marchini@unicam.it.

[†] These authors contributed equally to this work.

Keywords: gold compounds, phosphane, breast cancer, anticancer agents, apoptosis, proteasome inhibitors

Abstract

Basal like breast cancer (BLBC) is a very aggressive subtype of breast cancer giving few chances of survival, against which cisplatin based therapy is a compromise among the anticancer activity, the resistance development and the severe side effects. With the aim of finding new anticancer agents alternative to cisplatin, seven gold(I) azolate/phosphane compounds were evaluated *in vitro* by MTT tests in human MDA-MB-231, human mammary epithelial HMLE cells overexpressing FoxQ1, and murine A17 cells as models of BLBC. Two compounds, (4,5-dichloro-1H-imidazolate-1-yl)-(triphenylphosphane)-gold(I) **1** and (4,5-dicyano-1H-imidazolate-1-yl)-(triphenylphosphane)-gold(I) **2** were found very active and chosen for an *in vivo* study in A17 tumors transplanted in syngeneic mice. The compounds resulted to be more active than cisplatin, less nephrotoxic and generally more tolerated by the mice. This study also provides evidence that both gold(I) complexes inhibited the 19S proteasome-associated deubiquitinase USP14 and induced apoptosis, while compound **1**'s mechanism of action depends also on its ability to down-regulate key molecules governing cancer growth and progression, such as STAT3 and Cox-2.

Introduction

Basal-like Breast Cancer (BLBC) is one of the most aggressive subtypes of breast cancer and it is associated with the worst prognosis. BLBCs lack the expression of steroid hormone receptors (estrogen receptor and progesterone receptor) and human epidermal growth factor receptor 2, limiting targeted therapeutic options.[1] BLBC treatment usually consists of conventional cytotoxic chemotherapy: although patients are quite sensitive in the preoperative setting, they are nevertheless associated with short relapse-free and overall survival.[2,3] Hence, the development of new therapies with improved therapeutic indices is of paramount importance. In the search of anticancer drugs, metal-based drugs gained great importance starting from the accidental discovery of cisplatin, one of the leading agents in clinical use.[4] Preclinical and clinical data reveal encouraging activity of platinum-based chemotherapy drugs in BLBC,[5] however, their continued use is greatly limited by severe dose limiting side effects and intrinsic or acquired drug resistance.[6] Among all the drugs containing metals other than platinum, gold compounds have turned out to be a cutting-edge class of anticancer compounds.[7,8] Among all the classes of gold compounds,[8,9] the gold(I) phosphane complexes are potential good candidate for the anticancer therapy.[10,11] In fact, Auranofin (ridaura), an old and reliable anti-rheumatic drug, made of a tetracetylthioglucose and the gold(I)triethylphosphane fragment, [(2,3,4,6-tetra-O-acetyl-1-thio-β-D-glucopyranosato-S-[triethylphosphine]gold), has been recently reconsidered for the treatment of P388 leukemia,[12,13] lung's non small cell tumors,[14,15] as well as, in combination with other drugs, for the treatment of breast cancer.[16] A strong encouragement to continue the investigation in the anticancer activities of phosphane gold(I) complexes comes from the upgrade in the understanding of the mechanism of action of Auranofin and its derivatives.[17-19] Seleno-proteins such as Thioredoxine Reductase, were invested to possess a key role in a complicate network of biological processes[20,21] involving redox metabolism and mithocondria and, even if they have been identified as the major targets of gold(I) phosphane complexes[22] contextually the concept that gold compounds are multitarget

drugs grew up too.[19,23,24] The nature of the ligand, its slight modification as well as the gold coordination environment lead to the activation of preferential cellular paths.[19,25-27] However, Auranofin appears to have predominant antimitochondrial activity due to the inhibition or uncoupling of oxidative phosphorylation by gold(I) phosphine complexes; comparing its activity to those of cationic ([Au(dppe)$_2$]Cl) and ([Au(dppy)$_2$]Cl) (dppe = bis(diphenylphosphino)ethane, dppy = bis(dipyridylphosphino)ethane) complexes, showing a similar mechanism, the fine tuning of the hydro/lipophilic balancing gained attention in the gold drug design.[28] Azolate gold(I) phosphane complexes were found to possess a pronounced cytotoxic activity on many human cancer cells, some of which were endowed with cisplatin or multidrug resistance.[29,30] These compounds were made with pyrazolate or imidazolate and gold(I) triphenylphosphane or gold(I)TPA (TPA=1,3,5-triazaphosphaadamantane): for these latter a lack of activity was observed. Thus, assuming the hydro/lipophilicity might be the critical aspect on the design of effective anticancer gold(I) phosphane complexes with low systemic toxicity, planning N-Au-P or P-Au-Cl skeletal structure, different polar functional groups have been introduced either in the phosphane or/and in the azole ligand. Hence, a series of gold(I) complexes containing, in the azolate and/or in the phosphane ligand, polar groups such as COOH, CH_2OH, Cl, CN, were synthesized and labelled as follow: (4,5-dichloro-1H-imidazolate-1-yl)-(triphenylphosphane)-gold(I) **1**, ((4,5-dicyano-1H-imidazolate-1yl)-(triphenylphosphane)-gold(I) **2**, (2-benzoic acid-diphenylphosphane)-gold(I)chloride **3,** (4,5-dicyano-imidazolyl-1yl)-(4-benzoic acid-diphenylphosphane)-gold(I)) **4**, (4-Benzoic acid-diphenylphosphane)-gold(I)chloride) **5**, (4-hydroximethyl-imidazolyl-1yl)-(2-benzoic acid-diphenylphosphanegold(I) **6** and [tris(4-benzoic-diphenylphosphane-acid)-gold(I)chloride] **7**. Then, our goals have been: (i) to define the Structure Activity Relationship (SAR) of the above mentioned complexes; (ii) to evaluate their anticancer efficacy *in vitro*; (iii) to confirm their antitumor potential *in vivo* against a murine BLBC transplanted in a syngeneic host; and (iv) to investigate the mechanisms underlying their anticancer activity. Among all the complexes, we identified compounds **1** and **2** as the most powerful antitumor agents behaving as multi target anticancer agents.

Material and Methods

Synthesis of gold(I) phosphane complexes

For the synthesis, 2-benzoic acid of diphenylphosphine, 4-benzoic acid of diphenylphosphine and other chemicals were purchased and used without further purification. The complex Ph_3PAuCl was synthesized from tetrachloride gold (III) acid and a double molar amount of PPh_3 in ethyl alcohol as previously reported.[31] Solid Me_2SAuCl was synthesized by reducing $HAuCl_4$ with an excess of Me_2S and by washing with methanol the white solid obtained. Melting Points were not determined because most of the compounds decompose at low temperature and the meltings were not clearly observed. (4,5-dichloro-1H-imidazolate-1-yl)-(triphenylphosphane)-gold(I) **1**, (4,5-dicyano-1H-imidazolate-1yl)-(triphenylphosphane)-gold(I) **2**, (2-benzoic acid-diphenylphosphane)-gold(I)chloride **3** and (4,5-dicyano-imidazolyl-1yl)-(4-benzoic acid-diphenylphosphane)-gold(I)) **4**, (4-Benzoic acid-diphenylphosphane)-gold(I)chloride) **5** were synthesized as described in literature.[29,30] Samples for microanalysis were dried under vacuum (20°C, 0.1 torr) till constant weight. C, H and N elemental analyses were performed by the CARLO-ERBA ELEMENTAL ANALYSIS mod. 1106 mycro analyser at University of Camerino. Infrared spectra (4000 – 100 cm^{-1}) were recorded with PERKIN-ELMER SYSTEM 2000 FT-IR spectrophotometer. ^1H NMR spectra were recorded on an Oxford-400 Varian spectrometer. Chemical shifts, in ppm, for ^1H NMR spectra are relative to internal Me_4Si. Melting points were determined with an instrument ELECTROTHERMAL ENGINEERING LTD Mod.9100. Mass spectra (ESI-MS) were obtained for negative ions through HP Series 1100 MSD spectrometer. Solutions (ca. 0.1 mM) were prepared using MeOH as solvent. The experimental conditions were as following: the organic phase flow was 300 µL/min, the drying gas flow (N_2) was 10 L/min, the nebulization pressure was 30 psig, the temperature of the drying gas was 350 °C, the value for the fragmentor was fixed to 30, the acquisition of the data was performed by scanning in ranges from 500 to 2000 amu.

Synthesis of 4-hydromethyl)imidazolyl-1H-gold(I)-(2-benzoic-diphenylphosphane acid (compound 6)

50 mgs of solid 4-hydromethyl-imidazole (0.5 mmol) were dissolved in 5 mL of CH_3OH. To this solution 0.5 mL of a 1 M methanolic solution of KOH (0.5 mmol) were added. After magnetic stirring of a half of hour at room temperature, 12 mL of a methanolic solution containing 275 mgs of 2-benzoic-diphenylphosphaneacid-gold(I)-chloride were added (0.5 mmol). The suspension was stirred for two hours and then filtered off over a

celite bed. The clear solution was concentrated to 10 mL and let to evaporate till a microcrystalline solid was obtained Yield 63 %. M. p. 195-197°C.

^{1}H-NMR (CD_3OD, δ): 8.11 (s, br 1H); 7.65-7.46 (m, 13H), 7.41 (t, 1H), 7.00 (s, 1H), 6.86 (t, 1H), 4.56 (s, 1H) ^{31}P-NMR (CD_3OD, δ): 33.21 (s). MIR (cm^{-1}): 3123 (s, br), 3055 (m, br), 2855 (m, br), 1702.9 (vs), 1596 (s), 1579 (s), 1557 (s), 1479 (m), 1435 (s), 1371 (s), 1280 (m), 1256 (m), 1241 (m), 1206 (w), 1157 (w), 1101 (s), 1063 (w), 1019 (m), 982 (m), 937 (m), 879 (m-w), 830 (s), 747 (s), 710 (s), 692 (vs). FIR (cm-1): 555 (m), 519 (m), 543.6 (m-s), 500.8 (w), 433.8 (m), 393 (m), 285.7 (m), 227 (w), 175.6 (m), 153.4 (w), 135 (w). ESI (-) (CH_3OH, m/z) : 98 (45), 392 (30), 536.9 (100). ESI (+) (CH_3OH, m/z): 809 (100) $[(2\text{-}COOH\text{-}Ph_2P)_2Au]^+$. Elemental analysis for $C_{23}H_{20}AuN_2O_3P$, calcd %: C 46.01, H 3.36, N 4.67. Found C 46.56, H 4.01, N 4.99.

Synthesis of tris(4-benzoic-diphenylphosphane-acid)-gold(I)chloride (compound 7)

The solution of 4-(diphenylphosphine)benzoic acid (208.3mg; 0.4 mmol) in $CHCl_3$ was added dropwise to the solution of dimethylsulfidegold(I)chloride (30 mg; 0.1 mmol) in $CHCl_3$ (3 mL) at 0˚C The mixture was stirred at r. t. overnight. A pale yellow precipitate was obtained. The suspension was filtered off through a gooch. The solid was washed with few mL of $CHCl_3$ and dried by vacuum. The crude product was crystallized dissolving in few mL of $CHCl_3$ and adding cyclohexane.

Yield. 86%. M. p. 139-140˚C

^{1}H-NMR (CD_3OD, δ): 7.81 (d, 6H); 7.50 (t, 6H), 7.26 (m, 30H). ^{31}P-NMR (CD_3OD, δ): 42.09(s). MIR (cm^{-1}): 3484 (s, br), 3054 (m, br), 1702.9 (vs), 1597.9 (s), 1560.2 (s), 1481 (m), 1434 (s), 1393 (s), 1310.9 (m), 1275 (m, sh), 1225 (vs), 1183 (s),1122.6 b(m), 1091.8 (s), 1025.9 (m), 1016.8 (s), 998.9 (m), 855 (m-w), 791.9 (m), 764 (s, sh), 742.8 (s), 689.9 (vs).FIR (cm^{-1}): 534 (w), 513.5 (m), 367.8 (w), 295.68 (w), 176.95 (m), 139 (m), 125.7 (m), 106 (w), 58.43 (m), 39.8 (m). ESI (-) (CH_3OH, m/z) : 305.2 (100), 536.9 (40). ESI (+) (CH_3OH, m/z): 808.9 (100) $[(2\text{-}COOH\text{-}Ph_2P)_2Au]^+$. Elemental analysis for $C_{57}H_{51}AuClO_9P_3$, calcd %: C 56.80 , H 4.26. Found C 56.86, H 4.13.

Cell cultures

A17 cells were established from spontaneous lobular carcinomas that arose in a FVB/neuT mice transgenic for the activated form of rat HER-2/neu oncogene (FVB/neuT233), as previously described.[32,33] A17 cells were cultured in Dulbecco's Modified Eagle Medium (DMEM, Invitrogen, Carlsbad, CA) supplemented with 20% fetal bovine serum (FBS, Invitrogen, Carlsbad, CA) and 1% penicillin-streptomycin (P/S, Invitrogen, Carlsbad, CA). MDA-MB-231 cells were obtained from American Type Culture Collection (Rockville, MD) and cultured in DMEM supplemented with 10% FBS and 1% P/S. MDA-MB-468 and HMLE/FoxQ1 cells were cultured in DMEM supplemented with 10% FBS, 1% P/S or DMEM/HAM F12 (1:1) supplemented with 10% FBS, 1% P/S, 2 mM L-glutamine, 10 ng/mL human EGF, 0.5 µg/mL hydrocortisone and 10µg/mL insulin, respectively. To maintain the Foxq1 gene in HMLE/FoxQ1 cells, 2.5-5 µg/mL Blasticidin was added to culture media.[34], 30 Cells were grown in a humidified atmosphere with 5% CO_2 at 37°C.

Cell viability assay

The effects of gold(I) compounds (**1-7**), respect to cisplatin (cis-Diammineplatinum(II) dichloride, Sigma-Aldrich, St. Louis, MO), on cell viability were evaluated by seeding $2.5*10^3$ A17, $7*10^3$ MDA-MB-231, $7.5*10^3$ MDA-M-468 and $3*10^3$ HMLE/FoxQ1 cells/well in 96 wells plates in their respective complete medium. The day after, fresh medium containing appropriate concentrations of compounds **1, 2, 3, 4, 5, 6, 7** and cisplatin were added. After 24h and 48h, cell viability was determined using an MTT (Sigma Aldrich, St. Louis, MO) assay, as previously described.[35] The cytotoxicity of the compounds was reported as percentage of viable cells relative to control cells. All the experiments were repeated three times.

Immunoblotting analysis

Lysates were separated by 4-20% gradient precast SDS-PAGE (Bio-Rad) and transferred onto polyvinylidene difluoride (PVDF) membranes (Immobilion P, Millipore). For DUB labeling assay, cell lysates were incubated with Ub-VS for 30 minutes at 37°C, followed by boiling in reducing sample buffer and resolving by SDS-PAGE. For immunoblotting analysis on HMLE/Fox Q1 cell extracts, primary antibodies against NMNAT3 (D-10) (Santa Cruz Biotechnology, Inc.), Purified Mouse Anti-Human PARP (BD Pharmingen™), and USP14 (Abcam) were used, respectively. After secondary antibody incubation, the immunoreactive bands were captured

with ECL chemiluminescent substrates (Pierce Rockford) and detected by exposing to X-ray films (Kodak, Rochester, NY, USA). For immunoblotting analysis on tumor lysates, primary antibodies to β-actin, STAT3, phospho-STAT3, Cox-2, Slug and Snail were from Cell Signaling Technology. Secondary antibodies conjugated with peroxidase were from Sigma-Aldrich. The immunoreactive bands were detected by using LiteAblot PLUS (Euroclone) reagents and images were acquired with ChemiDoc Imaging System (Bio-Rad).

Animals

Female FVB mice, line 233, 6 weeks old, were obtained from Charles River S.r.l. (Lecco, Italy), and housed under controlled conditions. Mice were treated according to the European Community guidelines. The Animal Research Committee of the University of Camerino authorized the experimental protocol.

Treatments and tumor growth

A suspension of $1*10^5$ A17 viable cells in 200 µl of PBS was inoculated into mammary fat pad of 8-week-old FVB females. 10 days after tumor challenge, mice were randomly divided in 4 groups (5 mice per group) and treated with compound **1**, compound **2**, cisplatin or isotonic solution by intraperitoneal injection (via i.p.) in accordance with a treatment schedule (protocol q3x4) previously reported.[36] Briefly, 3 mg/kg/day of each compound (12 mg/kg final amount) were administered four times, once every three days. Body weight of mice and tumor growth was checked constantly until the end of the experiment, progressively growing masses >1 mm mean diameters were considered as tumors. Tumor volume was calculated as $0.5 \times d_1^2 \times d_2$, where d_1 and d_2 are the smaller and larger diameters, respectively. Tumors were surgically removed on day 24.

Histology and immunohistochemistry

Tumors and kidneys were harvested at the end of the experimental period, fixed in formalin and embedded in paraffin or fixed in PFA 4% and frozen in cryo-embedding medium (OCT Bioptica, Milan, Italy). To detect possible organ toxicity, kidney slides were stained with hematoxylin and eosin. Histopathological evidences of acute tissue damage were semi-quantified according to the methodology described elsewhere.[37] Two slides were analyzed in a blind fashion evaluating the following parameters: atrophic glomerulus, dilated proximal convoluted tubule, degenerated tubules, inflammatory cells infiltrate, desquamation of epithelial cells and cast

formation. The severity and incidence of each parameter was scored as follows: - absent , -/+ scarcely; +/- moderately; + frequently. For immunohistochemistry, tumor slides were incubated with the following primary antibodies: anti-CD31 (550274) and anti-CD105 (550546) (BD Pharmingen, Milan, Italy). After washing, slides were overlaid with appropriate secondary antibodies. Immunostaining was developed with DAB Chromogen System (Dako, Milan, Italy) or Vulcan Fast Red (Biocare, Milan, Italy) alkaline phosphatase method. The number of CD31/105 positive vessels was evaluated on digital images of controls, cisplatin, compound **1** and compound **2** treated tumors (5 per group, 5 x 400 microscopic fields per tumor).

Metal trace examination

Gold and platinum content in explanted kidneys from mice treated with compound **1**, compound **2**, cisplatin or isotonic solution was evaluated by ICP-MS. All solutions were prepared using ultrapure water obtained from a Millipore Milli-Q system (resistivity 18.2 MΩ cm). Optimized digestion of samples was carried out in a microwave digestor (Berghof Speedwave four, Berghof, Eningen, Germany) with 5 ml of HNO_3 (65%). Fifty microliters of iridium solution (20 mg) was added as recovery standard. Digested solutions were diluted with ultrapure water to obtain a solution with the correct acid concentration in order to perform analysis. The concentrations of metals in the processed samples were measured by ICP-MS (7500cx series) with the operating conditions described elsewhere.[38] Calibration curves were obtained using aqueous standard solutions (1,5% nitric acid) with appropriate stock standards dilutions (Fluka Analytical, Aldrich, Milan, Italy).

Step	1	2	3	4
T (° C)	150	190	50	50
P (bar)	36	36	0	0
Power (%)	70	90	0	0
Ramp (min)	5	5	1	1
Step (min)	10	20	15	1

Table 3) Optimized digestion protocol for explanted kidneys.

Proteasomal chymotrypsin-like activity in HMLE/FoxQ1 breast cancer cells

The HMLE/FoxQ1 cells were treated with compound **1** and compound **2** for different periods of time (0, 30, 60, 90, 120, 150, 180 minutes), lysed, and the protein concentrations were measured using a Bio-Rad protein assay (Bio-Rad). Whole-cell lysates (10 μg) were incubated for 2 h at 37℃ in 100 μl assay buffer (20 mM Tris-HCl, pH 7.5) with 20 μM fluorogenic peptide substrate Suc-LLVY-AMC (AnaSpec, Fremont, CA, USA). Proteasomal CT-like activity was measured using the Wallac Victor3 multi-label counter with an excitation lter of 365 nm and an emission filter of 460 nm, as previously described.[39]

Statistical analysis

Quantitative data are presented as means ± SEM from three independent experiments. The significance of differences was evaluated with two-tailed Students t test, or one way ANOVA followed by Bonferroni or Tukey's Multiple Comparison post test. Statistical analysis was executed with GraphPad Prism Software (San Diego, CA, USA), using $p<0.05$ as the critical level of significance (*$p \leq 0.05$; **$p \leq 0.01$; *** $p \leq 0.001$).

Results

Structure of the compounds

A set of gold(I) compounds having the N-Au-P or P-Au-Cl backbones were synthesized according to a general scheme where the azolate salt was treated with the selected phosphane gold(I) chloride or tetrafluoborate (Figure 1). It is known that compounds having a N-Au-P environment are more active than those with a C-Au-P chemical structure. Thus, the gold(I) compounds **1, 2**, **3** and **6** have the N-Au-P chemical backbone but, **c**ompounds **1** and **2** contain polar groups such as chloride and cyano groups in the imidazole ring and they have PPh_3 as coligand, compound **3** and **6** possess one COOH group in the phosphane ligand for the former and a CH_2OH group in the imidazole for the latter. Compounds **4** and **5** exhibit a P-Au-Cl backbone and they differ for the position of the COOH group in the phenyl group of the phosphane ligand (compound **4**, ortho position, and compound **5**, para position); lastly, the compound **7** contains the P-Au-Cl environment with the gold coordinated to three 4-benzoic diphenylphosphane ligands. The white microcrystalline solids of compounds **1**-**7** were prepared and used to prepare fresh stock solutions for the biological tests.

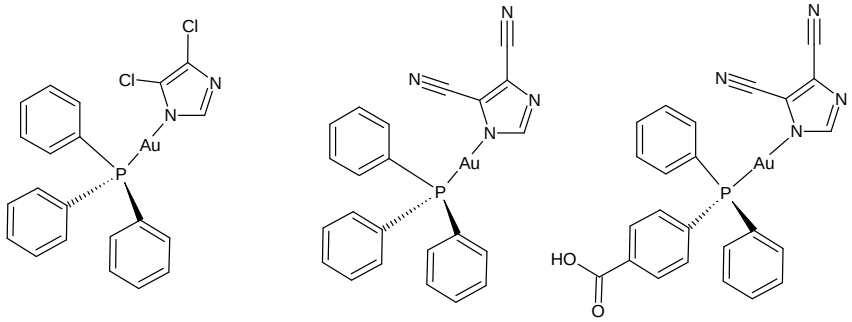

Compound **1** Compound **2** Compound **3**

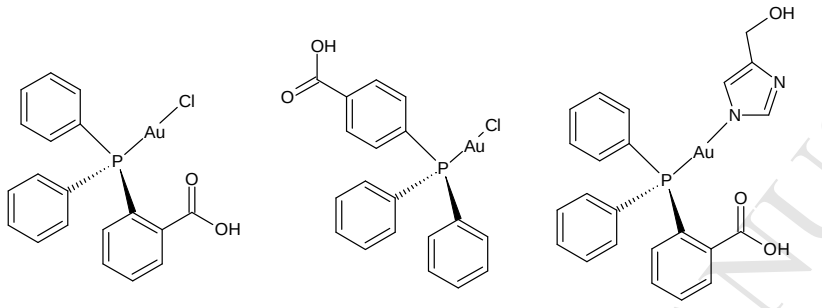

Compound **4** Compound **5** Compound **6**

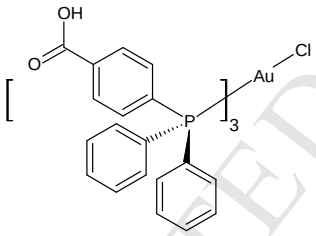

Compound **7**

Figure 1. Schematic representation of the gold(I) compounds tested in this work.

Compounds 1 and 2 inhibited BLBC growth *in vitro*

The effect of the new gold(I) compounds (**1-7**), compared with that of cisplatin, on cancer cell viability was estimated by MTT assay at 24h treatment using the human MDA-MB-231 cells and the murine A17 cells as models of BLBC.[40] Among the tested drugs, only compounds **1** and **2** exhibited a remarkable *in vitro* anticancer efficacy against both murine and human cell lines, being able to decrease cell viability in a dose-dependent manner with IC_{50} values at low µM concentrations, whereas compounds **3-7** failed in reducing significantly cell

viability even at the highest tested dose (Table 1; supporting information Figure 1, 2). Interestingly, compounds **1** and **2** displayed a stronger antineoplastic activity respect to cisplatin. In particular, the response of MDA-MB-231 cells to compounds **1** and **2** resulted to be stronger and even faster than that to cisplatin. In fact, compounds **1** and **2** showed IC_{50} values of 19.28 µM and 14.83 µM, respectively, after 24h treatment, whereas cisplatin displayed an IC_{50} value of 50.49 µM only after a 48h treatment (Table 1). In addition, *in vitro* screening was completed evaluating the cytotoxicity of the separate moieties of compounds **1** and **2**, corresponding to free azoles ($ImH(Cl)_2$ and $ImH(CN)_2$ for compounds **1** and **2**, respectively**)**, and triphenylphosphane moieties *(*Ph_3PAuCl and the bare Ph_3P) (supporting information Figure 4). Of note, only Ph_3PAuCl moiety was able to decrease viability in both A17 and MDA-MB-231 cells at 24h, with an IC_{50} value of 22.27 µM and 18.29 µM, respectively. On the contrary, $ImH(Cl)_2$, $ImH(CN)_2$ and Ph_3P displayed negligible cytotoxicity in both BLBC cells highlighting the role of the metal centre in the anticancer activity of our gold compounds **1** and **2** (supporting information Figure 3). The anticancer efficacy of compounds **1** and **2** was also confirmed on two other *in vitro* models of breast cancer: the human BLBC MDA-MB-468 cells[41] and human mammary epithelial HMLE cells overexpressing FoxQ1, characterized by stemness traits and chemoresistance.[34,42] HMLE/FoxQ1 line revealed to be the most responsive cells to both compound **1** and **2**, displaying IC_{50} values of 7.41 µM and 9.27 µM at 24h, respectively. Of note, cisplatin was less effective than compounds **1** and **2** also in HMLE/FoxQ1 and MDA-MB-468 cells, inducing a significant decrease in cellular viability only after 48h treatment with an IC_{50} value of 34.12 µM in HMLE/FoxQ1, and after 24h treatment with an IC_{50} value of 32.50 µM in MDA-MB-468 cells (Table 1; supporting information Figure 3).

Table 1- IC_{50} Values of Compounds 1−2, cisplatin on A17, MDA-MB-231, MDA-MB-468 and HMLE/FOXQ1 breast cancer cells.

Compound	Cell Line	Time	IC_{50} Mean ± SD[a] [µM]

Compound 1	A17	24h	11.38 ± 1.05
	MDA-MB-231	24h	19.28 ± 1.06
	MDA-MB-468	24h	13.62 ± 1.05
	HMLE/ FoxQ1	24h	7.41 ± 1.06
Compound 2	A17	24h	11.95 ± 1.04
	MDA-MB-231	24h	14.83 ± 1.05
	MDA-MB-468	24h	11.25 ± 1.14
	HMLE/FoxQ1	24h	9.27 ± 1.06
Cisplatin	A17	24h	15.86 ± 1.17
	MDA-MB-231	48h	50.49 ± 2
	MDA-MB-468	24h	32.50 ± 1.12
	HMLE/FoxQ1	48h	34.12 ± 2.17

[a] SD: standard deviation.

Table 1. Half Maximal Inhibitory Concentration (IC_{50}) values of compounds **1**,**2** and cisplatin for A17, MDA-MB-231, MDA-MB-468 and HMLE/FoxQ1 cells after 24h or 48h of treatment with increasing concentration of each gold(I) compound. IC_{50} values are expressed as Mean ± SD (μM).

Compounds 1 and 2 inhibited BLBC growth *in vivo*

We next investigated the *in vivo* antineoplastic effect of compounds **1** and **2**, which showed the strongest anticancer activity *in vitro*, against A17 cells, able to give rise to aggressive mesenchymal tumors when injected into syngeneic mice.[32,33] As previously described, A17 transplanted tumors share molecular signature with BLBC, including expression of vimentin, cytokeratin 14, N-cadherin and Cox-2.[40,43] The antineoplastic activity of compounds **1** and **2** was compared with that of cisplatin, known to be effective against A17 transplanted

tumors.[36] 10 days after tumor challenge when tumors became palpable, 3 mg/kg/day of each compound were administered 4 times, once every 3 days, in accordance with a previously reported protocol (q3X4).[36] Here we show that compounds **1** and **2** were able to reduce significantly A17 tumor growth. Of note, control tumors displayed a rapid growth rate, completely counteracted by both compounds **1**, **2** and cisplatin for all the duration of treatment (from day 10 to 19) (Figure 2A). In addition, both gold(I) compounds were able to significantly delay the growth of A17 tumors and to maintain them smaller than control ones even after the last drug administration (day 19) until the end of the experiment, although their effect was not long lasting as the cisplatin one (Figure 2A,B). Since A17 cells are able to give rise to highly vascularized aggressive tumors, we carried out histological and immunohistochemical analyses to evaluate the effect of compounds **1** and **2** on A17 tumor angiogenesis. In fact, several data support a central role for angiogenesis in breast cancer growth and metastasis.[44] Interestingly, both compound **1** and **2**, similarly to cisplatin, were able to provoke a reduction in the number of vessels (CD31/ 105 positive cells) in explanted tumors (supporting information Figure 5). Of note, body weight did not significantly differ in mice treated with compounds **1** and **2** respect to the control ones, suggesting that they have very low drug toxicity at the selected doses. On the contrary, cisplatin treated mice showed a continuous significant reduction in body weight during the treatment, reaching the maximum weight loss at day 19 (Figure 2C).

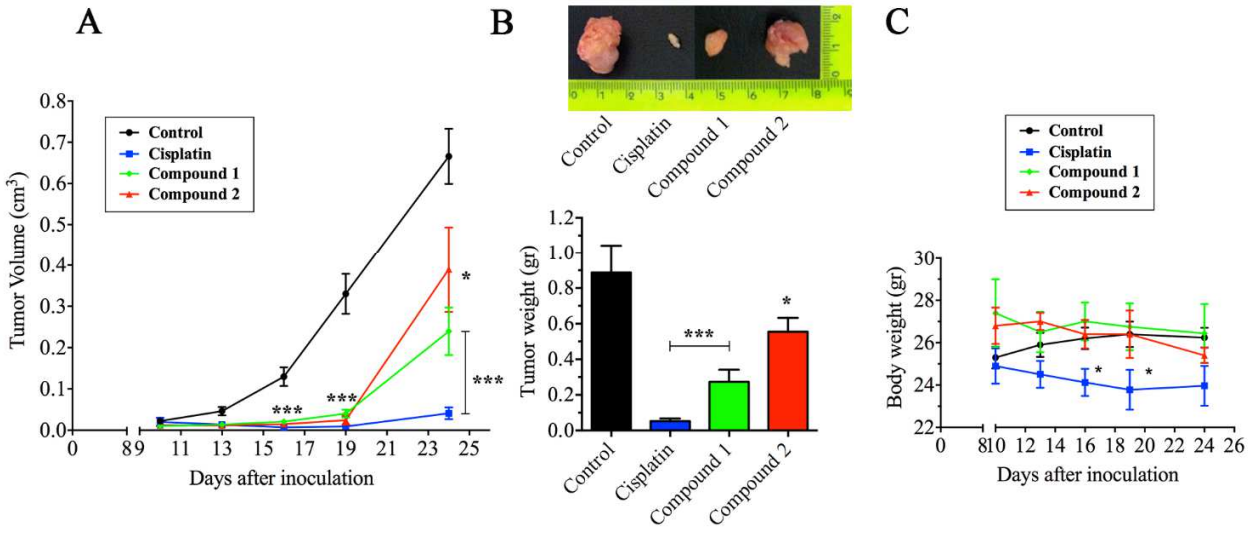

Figure 2. Compounds **1** and **2** suppressed BLBC growth *in vivo*. FVB female mice were injected with syngeneic A17 cells and treated with cisplatin, compound **1** or **2** or isotonic solution. Treatments schedule (q3x4) started ten days after cell injection. A) Tumor growth curves in mice receiving the treatment schedule q3X4. Values are mean ± SEM, n = 5/group; B) representative images of tumors explanted from control and treated mice at sacrifice (upper panel) and relative tumor weight (lower panel) 24 days after tumor challenge, values are mean ± SEM; C) effect of treatments on mean body weight of mice. Values are mean ± SEM. The significance was determined by the One way ANOVA test followed by Tukey's Multiple Comparison Post Test; each group was compared to control. (*$p \leq 0.05$; **$p \leq 0.01$; *** $p \leq 0.001$).

Compounds 1 and 2 exhibited reduced nephrotoxicity respect to cisplatin

To better evaluate the toxicity of compounds **1** and **2** we carried out an extensive histopathological analysis of explanted kidneys, common target organs of chemotherapy drugs. Importantly, hematoxylin and eosin (H&E) staining (Figure 3) and relative semiquantitive analysis (Table 2) revealed a significant reduced nephrotoxicity, similar for compound **1** and compound **2** treated mice, respect to cisplatin. In detail, histological changes in kidneys after cisplatin treatment revealed a severe atrophy of glomeruli, which was apparently due to the

reduction in its size, and moderate dilatation of proximal convoluted tubules with slogging of almost entire tubular epithelium due to its desquamation. Cisplatin treatment also provoked marked degeneration of tubules and moderate interstitial inflammatory cells infiltration (Figure 3 A,B,C) (Table 2). On the contrary, both compounds **1** and **2** administrations caused just a moderate atrophy of glomeruli respect to cisplatin, whereas the dilation of proximal convoluted tubule and the degeneration of tubules is comparable to controls. Interestingly, we revealed no signs of inflammation neither after compound **1** or compound **2** treatment (Figure 3 A,D,E,F) (Table 2). Furthermore, analysis of gold and platinum traces by Inductively Coupled Plasma-Mass Spectrometry (ICP-MS) analysis in the kidneys of treated mice clearly demonstrated a good excretion of both gold(I) phosphane compounds, significantly higher respect to cisplatin, that led to an accumulation of platinum in kidneys (Figure 4).

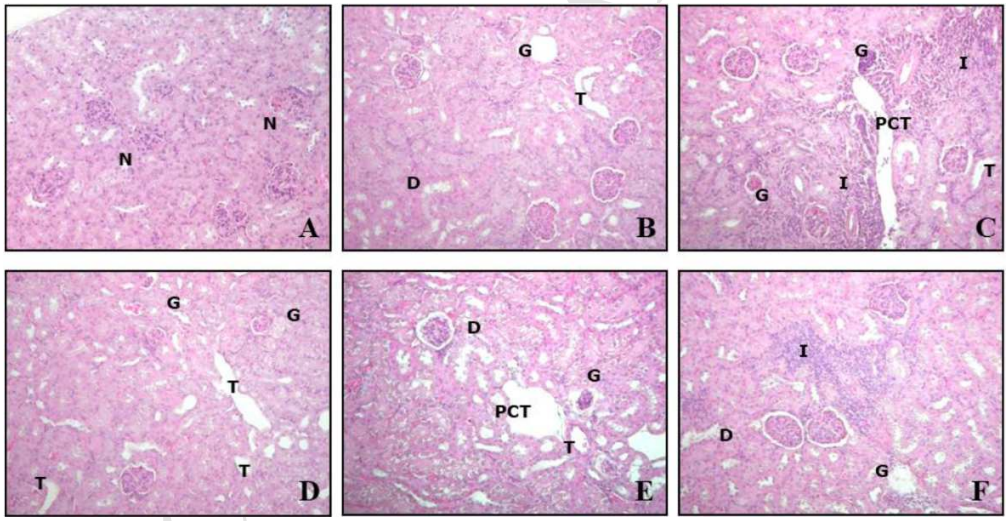

Figure 3. Histopathological effects of compound **1**, **2** and cisplatin in mouse kidney using hematoxylin and eosin (H&E) staining. A) Histology of normal control mouse kidney (isotonic solution); B,C) renal tissue of cisplatin-treated mice; D) renal tissue of compound **2**-treated mice; E,F): renal tissue of the compound **1**-treated mice. (N) normal glomeruli; (G) atrophic glomerulus; (PCT) dilated proximal convoluted tubule; (T) degenerated tubules; (I) inflammatory cells infiltrate; (D) desquamation of epithelial cells. (Magnification x 200).

	Isotonic solution score	Cisplatin score	Compound 1 Score	Compound 2 score
Atrophic glomerulus (G)	-/+	+	+/-	+/-
Dilated proximal convoluted tubule (PCT)	-/+	+/-	-/+	-/+
Degenerated tubules (T)	-/+	+	-/+	-/+
Inflammatory cells infiltrate (I)	-/+	+/-	-/+	-
Desquamation of epithelial cells (D)	-/+	+/-	+/-	+/-

Table 2. Semiquantitative analysis of histopathological features in kidneys after treatment with cisplatin, compound **1** and compound **2**: **-** absent , **-/+** scarcely; **+/-** moderately; **+** frequently.

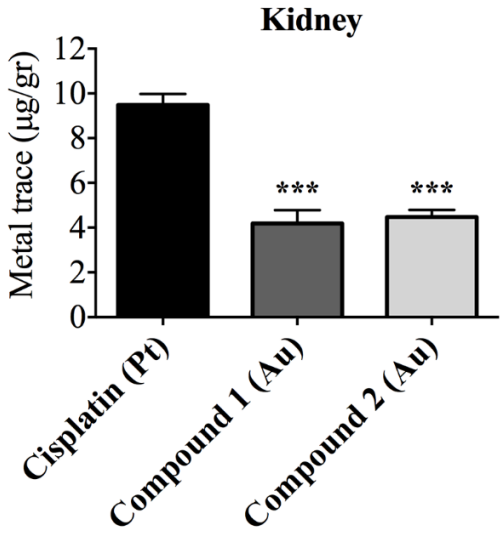

Figure 4. Gold and platinum content in kidneys of mice treated with compound **1**, compound **2** or cisplatin evaluated by Inductively Coupled Plasma-Mass Spectrometry (ICP-MS). The data are presented as micrograms of metal (Au or Pt) per gram of tissue. Values are mean ± SEM, n= 5/group. The significance was determined by the One way ANOVA test followed by Tukey's Multiple Comparison test (*** $p \leq 0.001$).

Compound 1 decreased Cox-2 expression in BLBC A17 transplanted tumors

A17 cells, beside the expression of mesenchymal markers, display constitutively active STAT3 transcription

factor[32,45] and overexpression of Cox-2, that is one of its downstream target genes.[43,46] Cox-2 is frequently associated with basal-like transcription pattern in human breast tumors,[40] where it correlates with their mesenchymal signature and their malignant phenotype regulating neoangiogenesis, invasion and anti-apoptotic mechanisms.[33,40,43,45,47] Thus, the molecular mechanisms underlying the anticancer effects of compound **1** and **2** were analysed by western blot firstly evaluating Cox-2 expression level in A17 tumors explanted from treated or untreated control mice. Our results show that both compound **1** and cisplatin treatments were able to induce a marked downregulation of Cox-2 expression, which was correlated with a significant decreased level of phospho-STAT3 (Figure 5). Furthermore, both compound **1** and cisplatin induced a significant reduction of both Snail and the closely related gene Slug (Figure 5), which mediate Epithelial Mesenchymal Transition (EMT) in invasive carcinoma cells and retain the mesenchymal aggressive phenotype.[43,47-50] On the contrary, compound **2** treatment did not affect neither Cox-2 expression nor STAT3 activation and it did not induce a decrease of Snail and Slug targets, suggesting a mechanism of action different from the one exerted by compound **1**.

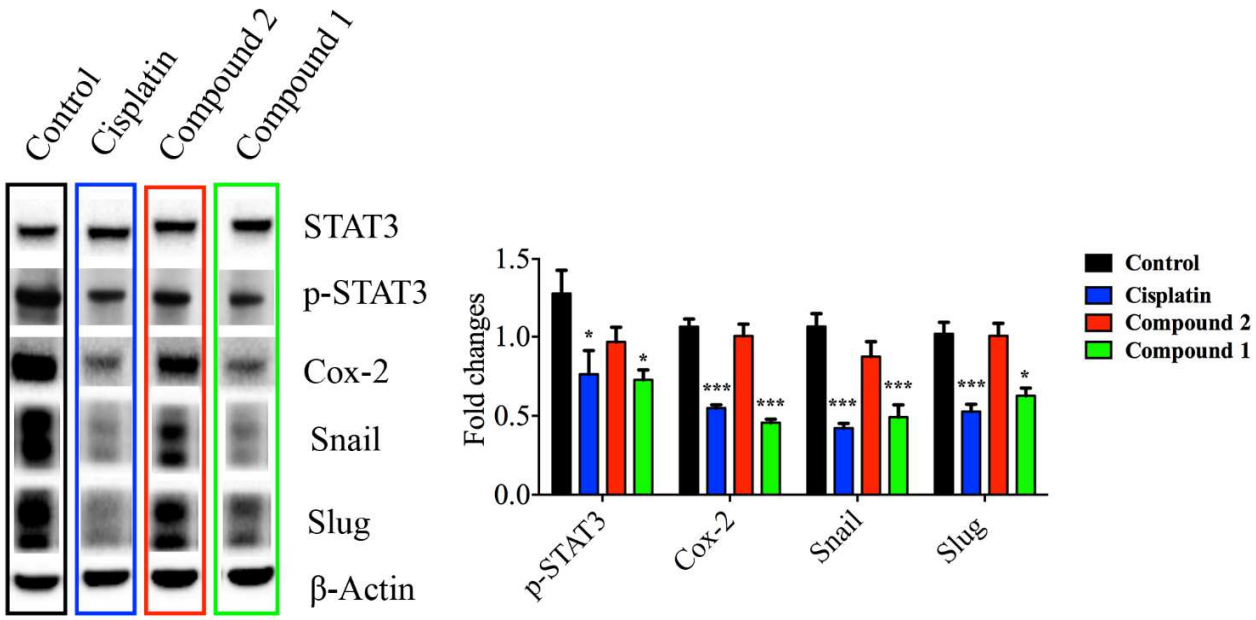

Figure 5. Effect of compound **1**, compound **2** and cisplatin treatment on STAT3 activation and Cox-2, Snail and Slug expression in A17 transplanted tumors. Representative image of western blot analysis (right panel) for the expression levels of STAT3, p-STAT3, Cox-2, Snail, Slug and β-actin (loading control) in A17 tumors from FVB mice receiving isotonic solution (control), compound **1**, compound **2** or cisplatin; densitometric quantification of p-STAT3, Cox-2, Snail and Slug expression normalized on β-actin (left panel) from three independent experiments, performed with ImageJ Software. Values are mean ± SEM. The significance was determined by the One way ANOVA test followed by Tukey's Multiple Comparison test (*$p \leq 0.05$; **$p \leq 0.01$; *** $p \leq 0.001$).

Compounds 1 and 2 were able to induce apoptosis in HMLE/FoxQ1 breast cancer cells

To gain further insights into the mechanism underlying anticancer activity of both compounds **1** and **2**, we investigated their ability to induce apoptosis in HMLE/FoxQ1 cells, which revealed the higher sensibility to both complexes *in vitro*, as previously described. Hence, HMLE/FoxQ1 cells were treated with compound **1** or compound **2** for 8h or 24h and cleavage of poly (ADP-ribose) polymerase-1 (PARP), a hallmark of apoptosis, was detected by western blot. Interestingly, both complexes were able to induce PARP cleavage after 8 to 24h treatment, suggesting their strong ability to trigger apoptosis in HMLE/FoxQ1 cells (Figure 6).

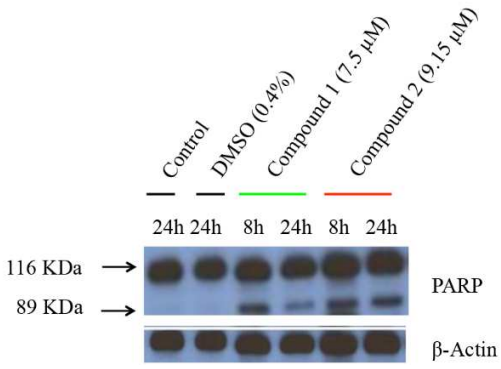

Figure 6. Compounds **1** and **2** induce apoptosis. Representative image of western blot analysis of PARP cleavage (89 kDa fragment) detected in HMLE/FoxQ1 cells upon treatment with compound **1** (7.5 µM) or compound **2** (9.15 µM), β-actin was used as loading control.

Compounds 1 and 2 induced accumulation of polyubiquitinated NMNAT3 (Nicotinamide mononucleotide adenylyltransferase 3) in HMLE/FoxQ1 breast cancer cells

Dou lab has found that NMNAT3 protein can be degraded by ubiquitin-proteasome system (unpublished results). NMNAT3 is the key enzyme in nicotinamide adenine dinucleotide (NAD) biosynthesis pathway in mitochondria and cancer cells generally display aberrant NAD metabolism, hence targeting NMNAT3 could be a strategy for treating different cancers. Thus, we investigated whether both compounds **1** and **2** had effect on the level of ubiquitinated NMAT3 in HMLE/FoxQ1 cells. Figure 7 showed that both gold(I) compounds were able to induce a time-dependent accumulation of polyubiquitinated NMNAT3 in treated HMLE/FoxQ1 cells, suggesting a possible inhibition of 26S proteasome either at 20S (proteolytic core) or 19S (regulatory part) via proteasome-associated deubiquitinases (DUBs) or both, leading to a block of degradation of ubiquitinated proteins and eventually to apoptosis. However, we excluded that our gold complexes could suppress tumor growth via direct inhibition of the 20S proteasome activity since they failed to inhibit 20S proteasomal enzymatic activity, measured by a proteasomal chymotrypsin-like (CT-like) assay in HMLE/FoxQ1 cells (data not shown).

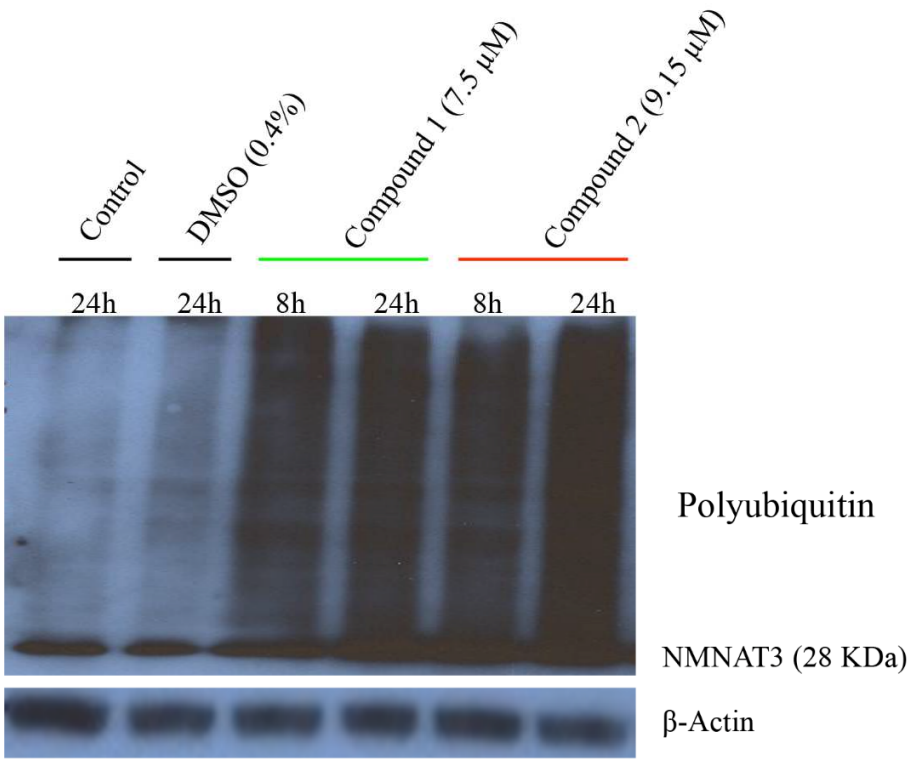

Figure 7. Effect of compounds **1** and **2** on ubiquitinated NMNAT3 in HMLE/FoxQ1 cells. Representative image of western blot analysis for the expression of ubiquitinated NMNAT3 was shown with β-actin as a loading control.

Compounds 1 and 2 inhibited 19S-associated Ubiquitin specific peptidase 14 (USP14) in HMLE/FoxQ1 breast cancer cells

Auranofin, a gold(I)-containing complex and a clinically used antirheumatic agent, has been found to be a proteasomal deubiquitinase inhibitor.[13] Since accumulation of polyubiquitinated NMNAT3 in HMLE/FoxQ1 cells treated with compounds **1** and **2** did not correlate with inhibition of 20S proteasomal enzymatic activity, we investigated their ability to inhibit the 19S proteasome-associated deubiquitinases (DUBs)[51] by UB-VS (Ubiquitin vinyl sulfone, HA-tag) assay. Interestingly, compounds **1** or **2** were able to partially inhibit 19S DUB USP14 after 1h and 3h treatment, as shown by the increased levels of unmodified USP14 protein (56 KDa) that indicates a competitive binding (Figure 8). However, after 5h treatment both gold(I) compounds treated cells

showed only the 66 kDa band (Ub-VS-bound form) which can be explained as decrease of inhibition of USP14 DUB.

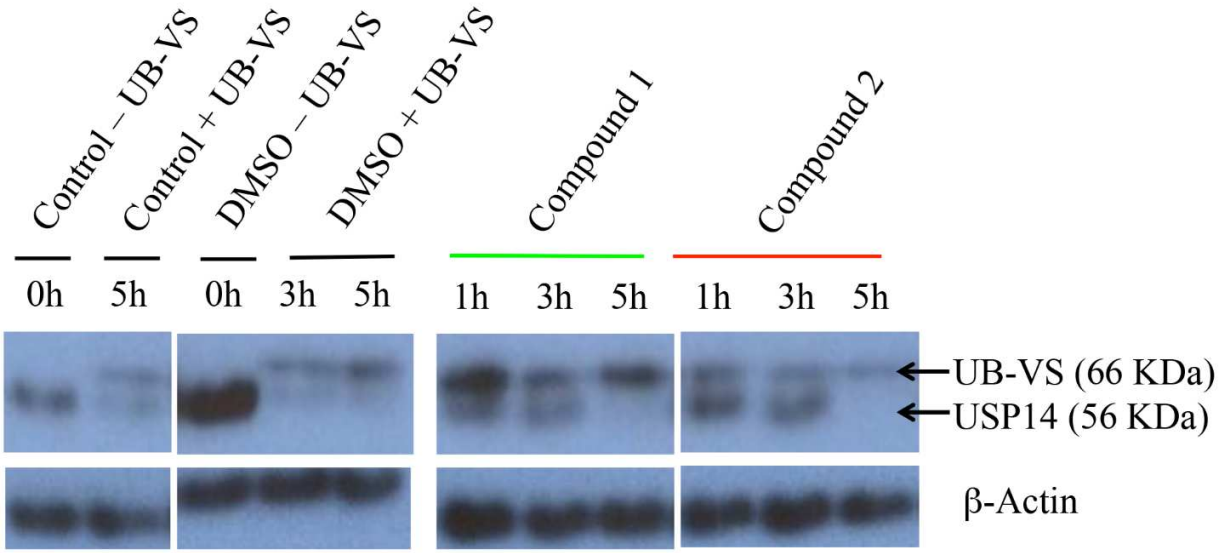

Figure 8. UB-VS (Ubiquitin vinyl sulfone, HA-tag) assay for USP14 in HMLE/FoxQ1 cells: ability of compound **1** and compound **2** to inhibit USP14. C–UB-VS= Control cells without UB-VS, C+UB-VS = Control cells with UB-VS, DMSO–UB-VS= DMSO without UB-VS, DMSO+UB-VS = DMSO with UB-VS, β-actin was used as loading control.

Discussion and conclusions

To date, BLBCs remain the most hard-to-treat breast tumor due to the lack of effective targeted therapies and the occurrence of resistance phenomena, which correlates with a short relapse-free and overall survival.[52] Experimental research on the promising cell growth inhibiting effects of gold(I) complex Auranofin, definitively triggered an immense interest in the research on gold complexes for cancer chemotherapy as innovative alternative metal based drug.[8] Hence in this work, seven new gold(I) complexes with different hydro/lipophilic properties have been screened for their anticancer activity against *in vitro* models of BLBC. Consistently, we found that micromolar concentration of compound **1** and compound **2** exhibited a unique *in vitro* dose-dependent cytotoxic activity, higher than cisplatin, against murine A17 cells and human MDA-MB-231 cells. Interestingly, the antitumor efficacy was confirmed also on both human MDA-MB-468 and HMLE/FoxQ1 BLBC cells, which resulted to be the most sensible cells to both gold compounds treatment. The *in vitro* cytotoxic activity of free azoles and phosphane moieties of compounds **1** and **2** was also assessed. Of note, just Ph_3PAuCl moiety possessed the ability to hamper cell growth *in vitro*, suggesting that the lipophilic fragment Ph_3PAu^+ is likely responsible for the antiproliferative activity. A structure–activity relationship study on 63 Auranofin analogues had already demonstrated the importance of the phosphine ligand as derivatives lacking this moiety were significantly less active.[53] These early evidences remark without any doubt that for this class of gold(I) compounds the introduction of hydrophilic groups such as the alcoholic or the carboxylic functions both in the azole and/or in the phosphane group hampers the expected anticancer activity, even though in literature is reported that hydrophilic phosphane gold(I) complex were found active against several panels of tumor cells.[54] Furthermore, the presence of polar groups (COOH) in only one of the aryl substituents of the phosphine cation, although it lowers the lipophilia and likely the side toxicity, negatively affects the anticancer activity, then the idea to lower the potential toxicity of the active PPh_3 moiety has to be forsaken. On the other hand, the presence of large and lipophilic ligand such as the phenyl group on the phosphorous guarantees a good cellular uptake.[25] In the present study, Ph_3PAuCl resulted to be less effective than compound **1** and compound **2** on both A17 and MDA-MB-231 cells at 24h treatment, suggesting that the introduction of azole ligands with polar functional

groups could be critical in determining the fate of anticancer properties of this new class of gold based drugs. Moreover, previous study on both Auranofin and the Et_3PAuCl, aimed to disclose the role of the Et_3PAu^+, showed that for the latter the DNA interaction was preferred[50,55] highlighting that the easier chloride exchange leads to alternative cellular path. So far, there have not been studies on the effects of compounds **1** and **2** in *in vivo* experimental tumor models. Hence, in this study we investigated the antineoplastic activity of both complexes against A17 transplanted tumors, representing a BLBC preclinical model. Of note, A17 cells are a highly tumorigenic and invasive cell line, established from an FVB/neuT transgenic mammary tumor, strongly related to human mesenchymal cancer stem cells and basal-like breast cancer.[33,40,45,47] Herein reported results indicate that both compound **1** and **2** administration was able to hamper BLBC tumor growth *in vivo*. Of note, the anticancer efficacy of both compounds **1** and **2** correlated with a reduced nephrotoxicity respect to cisplatin due to the increased hydrophilicity of the azolate gold(I) phosphane complexes which allowed a good excretion of gold from kidneys. Interestingly, the study performed on the molecular mechanisms underlying their anticancer effects suggests a different mechanism of action between compound **1** and compound **2**. Compound **1** induces a significant inhibition of STAT3 activation associated with a significant downregulation of Cox-2 expression. In fact, Cox-2 expression has been reported to be controlled by STAT3 transcription factor in A17 tumors.[45] This is a relevant result considering Cox-2 role in tumor growth, invasiveness and angiogenesis[56] and that a preferential activation of STAT3 has been reported in BLBC, where it seems to be specifically required for the maintenance of stem cell-like cancer cells.[57,58] Consistently, we found that phospho-STAT3 dowregulation induced by compound **1** correlates also with decreased levels of both Snail and Slug transcription factors, known to be involved in EMT. Thus, our data indicate that one of the main targets of compound **1** is STAT3 transcription factor, that represents a really good target for anticancer drugs conceived against BLBC, since its down-regulation leads to a decreased expression of key molecules governing cancer growth and progression, such as Cox-2 and the EMT inducers Slug and Snail.

On the contrary, probably due to a different structure of the whole molecule, the anticancer activity of compound **2** does not strictly depend on the same molecular targets affected by compound **1** suggesting a completely different mechanism of action which remains to be further examined. Furthermore, preliminary in vitro studies

on HMLE/FoxQ1 cells, allowed us to highlight alternative important mechanisms through which both compounds **1** and **2** could exert their anticancer activity *in vitro*. First, both gold(I) complexes induced apoptosis in HMLE/FoxQ1 cells as demonstrated by cleavage of PARP. The normal function of PARP is the routine repair of DNA damage, but it is also a preferred substrate for several 'suicidal' proteases. In fact, cleavage of PARP by caspases is considered to be a hallmark of apoptosis. Then, preliminary data suggest that the anticancer potential of these new gold(I) complexes is based on their ability to inhibit 19S associated DUBs, although a more in depth analysis of their mechanisms of action is necessary. In fact, compounds **1** and **2** targeted the deubiquitylating function of USP14, one of the DUBs associated with the proteasome 19S, leading to an accumulation of polyubiquitylated NMNAT3 in HMLE/FoxQ1 cells. Consistently, recent studies showed that some metal complexes, including gold(I) Auranofin, acting as inhibitors of 19S-associated DUBs UCHL5 and USP14, have promising antitumor effects.[51]

In conclusion, the present study demonstrates that compounds **1** and **2,** targeting key molecules associated with the malignant phenotype, provide an effective therapeutic strategy against BLBC associated with minimal side effects.

References

(1) Bertucci, F.; Finetti, P.; Birnbaum, D. Basal Breast Cancer: A Complex and Deadly Molecular Subtype. *Curr. Mol. Med.* **2012**, *12*, 96–110, doi: 10.2174/156652412798376134.

(2) André, F.; Zielinski, C. C. Optimal Strategies for the Treatment of Metastatic Triple-Negative Breast Cancer with Currently Approved Agents. *Ann. Oncol.* **2012**, *23 (suppl 6)*, 46-51.

(3) Apuri, S. Neoadjuvant and Adjuvant Therapies for Breast Cancer. *South. Med. J.* **2017**, *110*, 638–642, doi: 10.14423/SMJ.0000000000000703.

(4) Dasari, S.; Tchounwou, P. B. Cisplatin in Cancer Therapy: Molecular Mechanisms of Action. *Eur. J. Pharmacol.* **2014**, *740*, 364–378, doi: 10.1016/j.ejphar.2014.07.025.

(5) Silver, D. P.; Richardson, A. L.; Eklund, A. C.; Wang, Z. C.; Szallasi, Z.; Li, Q.; Juul, N.; Leong, C.-O.; Calogrias, D.; Buraimoh, A.; et al. Efficacy of Neoadjuvant Cisplatin in Triple-Negative Breast Cancer. *J. Clin. Oncol.* **2010**, *28*, 1145–1153, doi: 10.1200/JCO.2009.22.4725.

(6) Wheate, N. J.; Walker, S.; Craig, G. E.; Oun, R. The Status of Platinum Anticancer Drugs in the Clinic and in Clinical Trials. *Dalton Trans.* **2010**, *39*, 8113–8127, doi: 10.1039/C0DT00292E.

(7) Berners-Price, S. J.; Filipovska, A. Gold Compounds as Therapeutic Agents for Human Diseases. *Metallomics* **2011**, *3*, 863–873, doi: 10.1039/c1mt00062d.

(8) Ott, I. On the Medicinal Chemistry of Gold Complexes as Anticancer Drugs. *Coord. Chem. Rev.* **2009**, *253*, 1670–1681, doi: 10.1016/j.ccr.2009.02.019.

(9) Cinellu, M. A.; Ott, I.; Casini, A. Gold Organometallics with Biological Properties. In Bioorganometallic Chemistry; Jaouen, G., Salmain, M., Eds.; Wiley-VCH Verlag GmbH & Co. KGaA, **2014**, 117–140.

(10) Altaf, M.; Monim-ul-Mehboob, M.; Seliman, A. A.A.; Sohail, M.; Wazeer, M. LM.; Isab, A.A.; Dhuna, L.L.; Bhatia, G.; Dhuna K. Synthesis, characterization and anticancer activity of gold(I) complexes that contain tri-tert-butylphosphine and dialkyl dithiocarbamate ligands *Eur. J. Med. Chem.* **2015**, *95*, 464-472, DOI: 10.1016/j.ejmech.2015.03.019.

(11) Altaf, M.; Monim-ul-Mehboob, M.; Isab, A. A.; Dhuna, V.; Bhatia, G.; Dhuna, K.; Altuwaijri, S.; The synthesis, spectroscopic characterization and anticancer activity of new mono and binuclear phosphanegold(I) dithiocarbamate complexes *New J. Chem.*, **2015**, *39*, 377-385, DOI: 10.1039/c4nj00747f.

(12) Mirabelli, C. K.; Johnson, R. K.; Sung, C. M.; Faucette, L.; Muirhead, K.; Crooke, S. T. Evaluation of the in Vivo Antitumor Activity and in Vitro Cytotoxic Properties of Auranofin, a Coordinated Gold Compound, in Murine Tumor Models. *Cancer Res.* **1985**, *45*, 32–39.

(13) Fiskus, W.; Saba, N.; Shen, M.; Ghias, M.; Liu, J.; Gupta, S. D.; Chauhan, L.; Rao, R.; Gunewardena, S.; Schorno, K.; et al. Auranofin Induces Lethal Oxidative and Endoplasmic Reticulum Stress and Exerts Potent Preclinical Activity against Chronic Lymphocytic Leukemia. *Cancer Res.* **2014**, *74*, 2520–253, doi: 10.1158/0008-5472.CAN-13-2033.

(14) Li, H.; Hu, J.; Wu, S.; Wang, L.; Cao, X.; Zhang, X.; Dai, B.; Cao, M.; Shao, R.; Zhang, R.; et al. Auranofin-Mediated Inhibition of PI3K/AKT/mTOR Axis and Anticancer Activity in Non-Small Cell Lung Cancer Cells. *Oncotarget* **2016**, *7*, 3548–3558, doi: 10.18632/oncotarget.6516.

(15) Liu, N.; Li, X.; Huang, H.; Zhao, C.; Liao, S.; Yang, C.; Liu, S.; Song, W.; Lu, X.; Lan, X.; et al. Clinically Used Antirheumatic Agent Auranofin Is a Proteasomal Deubiquitinase Inhibitor and Inhibits Tumor Growth. *Oncotarget* **2014**, *5*, 5453–5471, doi: 10.18632/oncotarget.2113.

(16) Lee, J.-E.; Kwon, Y.-J.; Baek, H.-S.; Ye, D.-J.; Cho, E.; Choi, H.-K.; Oh, K.-S.; Chun, Y.-J. Synergistic Induction of Apoptosis by Combination Treatment with Mesupron and Auranofin in Human Breast Cancer Cells. *Arch. Pharm. Res.* **2017**, *40*, 746–759, doi: 10.1007/s12272-017-0923-0 10.1007/s12272-017-0923-0.

(17) Casini, A.; Messori, L. Molecular Mechanisms and Proposed Targets for Selected Anticancer Gold Compounds. *Curr. Top. Med. Chem.* **2011**, *11*, 2647–2660, doi: 10.2174/156802611798040732.

(18) Landini, I.; Lapucci, A.; Pratesi, A.; Massai, L.; Napoli, C.; Perrone, G.; Pinzani, P.; Messori, L.; Mini, E.; Nobili, S.; et al. Selection and Characterization of a Human Ovarian Cancer Cell Line Resistant to Auranofin. *Oncotarget* **2017**, *8*, 96062–96078, doi: 10.18632/oncotarget.21708.

(19) Zou, T.; Lum, C. T.; Lok, C.-N.; Zhang, J.-J.; Che, C.-M. Chemical Biology of Anticancer gold(III) and gold(I) Complexes. *Chem. Soc. Rev.* **2015**, *44*, 8786–8801, doi: 10.1039/c5cs00132c.

(20) Shaw, C. F.; Isab, A. A.; Hoeschele, J. D.; Starich, M.; Locke, J.; Schulteis, P.; Xiao, J. Oxidation of the Phosphine from the Auranofin Analogue, Triisopropylphosphine (2,3,4,6-tetra-O-acetyl-1-thio-β-D-glucopyranosato-S)gold(I), via a Protein-Bound Phosphonium Intermediate. *J. Am. Chem. Soc.* **1994**, *116*, 2254-2260.

(21) Hill, D. T.; Isab, A. A.; Griswold, D.E.; DiMartino, M. J.; Matz, E. D., Figueroa, A. L.; Wawro, J. E.; DeBrosse, C.; Reiff, W. M.; Elder, R. C.; Jones, B.; Webb, J. W., Shaw III, C. F. Seleno-Auranofin (Et_3PAuSe-tagl): Synthesis, Spectroscopic (EXAFS, ^{197}Au Mössbauer, ^{31}P, ^{1}H, ^{13}C, and ^{77}Se

NMR, ESI-MS) Characterization, Biological Activity, and Rapid Serum Albumin-Induced Triethylphosphine Oxide Generation. *Inorg. Chem.* **2010**, *49*, 7663–7675, 10.1021/ic902335z.

(22) Bindoli, A.; Rigobello, M. P.; Scutari, G.; Gabbiani, C.; Casini, A.; Messori, L. Thioredoxin Reductase: A Target for Gold Compounds Acting as Potential Anticancer Drugs. *Coord. Chem. Rev.* **2009**, *253*, 1692–170, doi: 10.1016/j.ccr.2009.02.026.

(23) Milacic, V.; Dou, Q. P. The Tumor Proteasome as a Novel Target for gold(III) Complexes: Implications for Breast Cancer Therapy. *Coord. Chem. Rev.* **2009**, *253*, 1649–1660, doi: 10.1016/j.ccr.2009.01.032.

(24) Chen, X.; Zhou, H. J.; Huang, Q.; Lu, L.; Min, W. Novel Action and Mechanism of Auranofin in Inhibition of Vascular Endothelial Growth Factor Receptor-3-Dependent Lymphangiogenesis. *Anticancer Agents Med. Chem.* **2014**, *14*, 946–954, doi: 10.2174/1871520614666140610102651.

(25) Scheffler, H.; You, Y.; Ott, I. Comparative Studies on the Cytotoxicity, Cellular and Nuclear Uptake of a Series of Chloro gold(I) Phosphine Complexes. *Polyhedron* **2010**, *29*, 66–69, doi: 10.1016/j.poly.2009.06.007.

(26) Messori, L. Scaletti, F. Massai, L. Cinellu, M. A. Gabbiani, C. Vergara, A., Merlino A. The mode of action of anticancer gold-based drugs: a structural perspective *Chem. Commun.***, 2013**, *49*, 10100-10102, doi: 10.1039/C3CC46400H.

(27) Ali, M.; Dondaine, L.; Adolle, A.; Sampaio, C.; Chotard, F.; Richard, P.; Denat, F.; Bettaieb, A.; Le Gendre, P.; Laurens, V.; et al. Anticancer Agents: Does a Phosphonium Behave Like a Gold(I) Phosphine Complex? Let a "Smart" Probe Answer*! J. Med. Chem.* **2015**, *58*, 4521–4528, doi: 10.1021/acs.jmedchem.5b00480.

(28) McKeage, M. J.; Maharaj, L.; Berners-Price, S. J. Mechanisms of Cytotoxicity and Antitumor Activity of gold(I) Phosphine Complexes: The Possible Role of Mitochondria. *Coord. Chem. Rev.* **2002**, *232*, 127–13.

(29) Galassi, R.; Burini, A.; Ricci, S.; Pellei, M.; Rigobello, M. P.; Citta, A.; Dolmella, A.; Gandin, V.; Marzano, C. Synthesis and Characterization of Azolate gold(I) Phosphane Complexes as

Thioredoxin Reductase Inhibiting Antitumor Agents. *Dalton Trans.* **2012**, *41*, 5307–5318, doi: 10.1039/c2dt11781a.

(30) Galassi, R.; Oumarou, C. S.; Burini, A.; Dolmella, A.; Micozzi, D.; Vincenzetti, S.; Pucciarelli, S. A Study on the Inhibition of Dihydrofolate Reductase (DHFR) from Escherichia Coli by Gold(i) Phosphane Compounds. X-Ray Crystal Structures of (4,5-Dichloro-1H-Imidazolate-1-Yl)-Triphenylphosphane-Gold(I) and (4,5-Dicyano-1H-Imidazolate-1-yl)-Triphenylphosphane-Gold(I). *Dalton Trans.* **2015**, *44*, 3043–3056, doi: 10.1039/C4DT01542H.

(31) Mann, F. G.; Wells, A. F.; Purdie, D. 386. The Constitution of Complex Metallic Salts. Part VI. The Constitution of the Phosphine and Arsine Derivatives of Silver and Aurous Halides. The Configuration of the Co-Ordinated Argentous and Aurous Complex. *J. Chem. Soc.* **1937**, 1828–1836.

(32) Galiè, M.; Sorrentino, C.; Montani, M.; Micossi, L.; Di Carlo, E.; D'Antuono, T.; Calderan, L.; Marzola, P.; Benati, D.; Merigo, F.; et al. Mammary Carcinoma Provides Highly Tumourigenic and Invasive Reactive Stromal Cells. C*arcinogenesis* **2005**, *26*, 1868–1878, doi: 10.1093/carcin/bgi158.

(33) Galiè, M.; Konstantinidou, G.; Peroni, D.; Scambi, I.; Marchini, C.; Lisi, V.; Krampera, M.; Magnani, P.; Merigo, F.; Montani, M.; et al. Mesenchymal Stem Cells Share Molecular Signature with Mesenchymal Tumor Cells and Favor Early Tumor Growth in Syngeneic Mice. *Oncogene* **2008**, *27*, 2542–2551, doi: 10.1038/sj.onc.1210920

(34) Zhang, H.; Meng, F.; Liu, G.; Zhang, B.; Zhu, J.; Wu, F.; Ethier, S. P.; Miller, F.; Wu, G. Forkhead Transcription Factor Foxq1 Promotes Epithelial–Mesenchymal Transition and Breast Cancer Metastasis. *Cancer Res.* **2011**, *71*, 1292–1301, doi: 10.1158/0008-5472.

(35) Daniel, K. G.; Chen, D.; Orlu, S.; Cui, Q. C.; Miller, F. R.; Dou, Q. P. Clioquinol and Pyrrolidine Dithiocarbamate Complex with Copper to Form Proteasome Inhibitors and Apoptosis Inducers in Human Breast Cancer Cells. *Breast Cancer Res.* **2005**, *7*, R897-908, doi: 10.1186/bcr1322.

(36) Montani, M.; Pazmay, G. V. B.; Hysi, A.; Lupidi, G.; Pettinari, R.; Gambini, V.; Tilio, M.; Marchetti, F.; Pettinari, C.; Ferraro, S.; et al. The Water Soluble Ruthenium(II) Organometallic Compound [Ru(p-cymene)(bis(3,5 Dimethylpyrazol-1-yl)methane)Cl]Cl Suppresses Triple Negative

Breast Cancer Growth by Inhibiting Tumor Infiltration of Regulatory T Cells. *Pharmacol. Res.* **2016**, *107*, 282–290, doi: 10.1016/j.phrs.2016.03.032.

(37) Dinis-Oliveira, R. J.; Duarte, J. A.; Remião, F.; Sánchez-Navarro, A.; Bastos, M. L.; Carvalho, F. Single High Dose Dexamethasone Treatment Decreases the Pathological Score and Increases the Survival Rate of Paraquat-Intoxicated Rats. *Toxicology* **2006**, *227*, 73–85, doi: 10.1016/j.tox.2006.07.025.

(38) Fantuz, F.; Ferraro, S.; Todini, L.; Mariani, P.; Piloni, R.; Salimei, E. Essential Trace Elements in Milk and Blood Serum of Lactating Donkeys as Affected by Lactation Stage and Dietary Supplementation with Trace Elements. *Animal* **2013**, *7*, 1893–1899, doi: 10.1017/S175173111300133X.

(39) Zhang P., Bi C., Schmitt S. M., Li X., Fan Y., Zhang N., Dou P.Q. Metal-based 2,3-Indolinedione Derivatives as Proteasome Inhibitors and Inducers of Apoptosis in Human Cancer Cells *Int J Mol Med.* **2014**, *34*, 870-879, doi: 10.3892/ijmm.2014.1838

(40) Marchini, C.; Montani, M.; Konstantinidou, G.; Orrù, R.; Mannucci, S.; Ramadori, G.; Gabrielli, F.; Baruzzi, A.; Berton, G.; Merigo, F.; et al. Mesenchymal/Stromal Gene Expression Signature Relates to Basal-like Breast Cancers, Identifies Bone Metastasis and Predicts Resistance to Therapies. *PloS One* **2010**, *5*, e14131, doi: 10.1371/journal.pone.0014131.

(41) Lehmann, B. D.; Bauer, J. A.; Chen, X.; Sanders, M. E.; Chakravarthy, A. B.; Shyr, Y.; Pietenpol, J. A. Identification of Human Triple-Negative Breast Cancer Subtypes and Preclinical Models for Selection of Targeted Therapies. *J. Clin. Invest.* **2011**, *121*, 2750–2767, doi: 10.1172/JCI45014.

(42) Meng, F.; Speyer, C. L.; Zhang, B.; Zhao, Y.; Chen, W.; Gorski, D. H.; Miller, F. R.; Wu, G. PDGFR and Play Critical Roles in Mediating Foxq1-Driven Breast Cancer Stemness and Chemoresistance. *Cancer Res.* **2015**, *75*, 584–593, doi: 10.1158/0008-5472.CAN-13-3029.

(43) Bisaro, B.; Montani, M.; Konstantinidou, G.; Marchini, C.; Pietrella, L.; Iezzi, M.; Galiè, M.; Orso, F.; Camporeale, A.; Colombo, S. M.; et al. p130Cas/Cyclooxygenase-2 Axis in the Control of

Mesenchymal Plasticity of Breast Cancer Cells. *Breast Cancer Res. BCR* **2012**, *14*, R137, doi: 10.1186/bcr3342

(44) Bujor, I.S.; Cioca, A.; Ceaușu, R.A.; Veaceslav, F.; Nica, C.; Cîmpean, A.M.; Raica, M. Evaluation of Vascular Proliferation in Molecular Subtypes of Breast Cancer. *In Vivo* **2018**, *32(1)*, 79-83, doi: 10.21873/invivo.11207.

(45) Kalogris, C.; Garulli, C.; Pietrella, L.; Gambini, V.; Pucciarelli, S.; Lucci, C.; Tilio, M.; Zabaleta, M. E.; Bartolacci, C.; Andreani, C.; et al. Sanguinarine Suppresses Basal-like Breast Cancer Growth through Dihydrofolate Reductase Inhibition. *Biochem. Pharmacol.* **2014**, *90*, 226–234, doi: 10.1016/j.bcp.2014.05.014.

(46) Yu, L.-J.; Wu, M.-L.; Li, H.; Chen, X.-Y.; Wang, Q.; Sun, Y.; Kong, Q.-Y.; Liu, J. Inhibition of STAT3 Expression and Signaling in Resveratrol-Differentiated Medulloblastoma Cells. *Neoplasia N. Y. N* **2008**, *10*, 736–744, doi: 10.1593/neo.08304.

(47) Garulli, C.; Kalogris, C.; Pietrella, L.; Bartolacci, C.; Andreani, C.; Falconi, M.; Marchini, C.; Amici, A. Dorsomorphin Reverses the Mesenchymal Phenotype of Breast Cancer Initiating Cells by Inhibition of Bone Morphogenetic Protein Signaling. *Cell. Signal.* **2014,** *26*, 352–361, doi: 10.1016/j.cellsig.2013.11.022.

(48) Peinado, H.; Portillo, F.; Cano, A. Transcriptional Regulation of Cadherins during Development and Carcinogenesis. *Int. J. Dev. Biol.* **2004**, *48*, 365–375, doi: 10.1387/ijdb.041794hp.

(49) Martin, T. A.; Goyal, A.; Watkins, G.; Jiang, W. G. Expression of the Transcription Factors Snail, Slug, and Twist and Their Clinical Significance in Human Breast Cancer. *Ann. Surg. Oncol.* **2005**, *12*, 488–496, doi: 10.1245/ASO.2005.04.010.

(50) Kang, Y.; Massagué, J. Epithelial-Mesenchymal Transitions: Twist in Development and Metastasis. *Cell* **2004**, *118*, 277–279, doi: 10.1016/j.cell.2004.07.011.

(51) Liu, N.; Huang, H.; Dou, Q. P.; Liu, J. Inhibition of 19S Proteasome-Associated Deubiquitinases by Metal-Containing Compounds. *Oncoscience* **2015**, *2 (5)*, 457-466, doi: 10.18632/oncoscience.167.

(52) Bertucci, F.; Finetti, P.; Birnbaum, D. Basal Breast Cancer: A Complex and Deadly Molecular Subtype. *Curr. Mol. Med.* **2012**, *12*, 96–110.

(53) Mirabelli, C. K.; Johnson, R. K.; Hill, D. T.; Faucette, L. F.; Girard, G. R.; Kuo, G. Y.; Sung, C. M.; Crooke, S. T. Correlation of the in Vitro Cytotoxic and in Vivo Antitumor Activities of gold(I) Coordination Complexes. *J. Med. Chem.* **1986**, *29*, 218–223.

(54) Pillarsetty, N.; Katti, K.K; Hoffman, T.J.; Volkert, W.A.; Katti, K.V.; Kamei, H.; Koide, T. In Vitro and In Vivo Antitumor Properties of Tetrakis ((trishydroxymethyl) phosphine)gold(I)chloride. *J. Med. Chem.* **2003**, *46*, 1130–1132, doi: 10.1021/jm025615g.

(55) Blank, C. E.; Dabrowiak, J. C. Absorption and Circular Dichroism Studies of a Gold (I)-DNA Complex. *J. Inorg. Biochem.* **1984**, *21*, 21–29, doi: 10.1016/0162-0134(84)85036-9.

(56) Singh-Ranger, G.; Salhab, M.; Mokbel, K. The Role of Cyclooxygenase-2 in Breast Cancer: Review. *Breast Cancer Res. Treat.* **2008**, *109*, 189–198, doi: 10.1007/s10549-007-9641-5.

(57) Marotta, L. L. C.; Almendro, V.; Marusyk, A.; Shipitsin, M.; Schemme, J.; Walker, S. R.; Bloushtain-Qimron, N.; Kim, J. J.; Choudhury, S. A.; Maruyama, R.; et al. The JAK2/STAT3 Signaling Pathway Is Required for Growth of CD44+CD24− Stem Cell-like Breast Cancer Cells in Human Tumors. *J. Clin. Invest.* **2011**, *121*, 2723–2735, doi: 10.1007/s10549-007-9641-5.

(58) Honeth, G.; Bendahl, P.-O.; Ringnér, M.; Saal, L. H.; Gruvberger-Saal, S. K.; Lövgren, K.; Grabau, D.; Fernö, M.; Borg, A.; Hegardt, C. The CD44+/CD24- Phenotype Is Enriched in Basal-like Breast Tumors. *Breast Cancer Res.* **2008**, *10*, R53, doi: 10.1186/bcr2108.

Ancillary Information

Supporting Information

Evaluation of antiproliferative activity of gold(I) phosphane complexes on different BLBC *in vitro* models by MTT assay (Figure S1-S4) and IHC analysis of angiogenesis in A17 tumors (Figure S5).

Corresponding Authors

Rossana Galassi, Tel:+39 0737 402243; Email: rossana.galassi@unicam.it;

Cristina Marchini, Tel: +39 0737 403275; Email: cristina.marchini@unicam.it.

Author Contibutions

Valentina Gambini, Martina Tilio (co-first authors) and Rossana Galassi, Augusto Amici (co-last authors) contributed equally to this work.

Acknowledgement

Eunice Wairimu Maina acknowledges the assistance of Claire Soave in the proteasomal chymotrypsin-like assay and University of Camerino for the abroad financial coverage (Bando Paesi Terzi 2016). Rossana Galassi is grateful to CIRCMSB (Consorzio Interuniversitario di Ricerca in Chimica dei Metalli nei Sistemi Biologici).

Highlights

- Seven phosphane/azolate gold(I) compounds were synthesized and SAR was determined.
- Two compounds (**1**: (4,5-dichloro-1H-imidazolate-1-yl)-(triphenylphosphane)-gold(I) and **2**: (4,5-dicyano-1H-imidazolate-1yl)-(triphenylphosphane)-gold(I)) induce apoptosis in basal-like breast cancer (BLBC) cells.
- Compounds **1** and **2** inhibit BLBC growth *in vivo*.
- Compounds **1** and **2** induce accumulation of polyubiquitinated NMNAT3.
- Compounds **1** and **2** inhibit 19S proteasome-associated deubiquitinase USP14.